Technical Paper

Journal of the Society of Naval Architects of Korea
Vol. 19, No. 4, December 1982

Finite-element Method for Heat Transfer Problem in Hydrodynamic Lubrication

by

Kwang June Bai*

Abstract

Galerkin's finite element method is applied to a two-dimensional heat convection-diffusion problem arising in the hydrodynamic lubrication of thrust bearings used in naval vessels. A parabolized thermal energy equation for the lubricant, and thermal diffusion equations for both bearing pad and the collar are treated together, with proper juncture conditions on the interface boundaries. It has been known that a numerical instability arises when the classical Galerkin's method, which is equivalent to a centered difference approximation, is applied to a parabolic-type partial differential equation. Probably the simplest remedy for this instability is to use a one-sided finite difference formula for the first derivative term in the finite difference method. However, in the present coupled heat convection-diffusion problem in which the governing equation is parabolized in a subdomain (lubricant), uniformly stable numerical solutions for a wide range of the Peclet number are obtained in the numerical test based on Galerkin's classical finite element method. In the present numerical computations, numerical convergence errors in several error norms are presented in the first model problem. Additional numerical results for a more realistic bearing lubrication problem are presented for a second numerical model.

Notations

A Constant in Error Representation
C Heat Capacity
E_i Error Norm Defined in Equation (13); ($i=1, \cdots, 4$)
f_i Known Function on Γ_i ($i=1$ and 3) in the Neumann Condition
h_i Heat Film Coefficient on Γ_i ($i=1$ and 3) in the Robin Condition
J Heat-Mechanical Energy Conversion Factor (=9336 in lbf/Btu)
J_i Juncture Boundary ($i=1, 2$)
k_i Thermal Conductivity in Ω_i ($i=1, 2, 3$)
L Length of Bearing Pad
n Index of Error
(Oxy) Rectangular Coordinate Defined in Figure 1
P_e Peclet Number
T Temperature in Fahrenheit
T_i Temperature in Subdomain Ω_1 ($i=1, 2, 3$)
T^* Test Function in Weak Formulation
$\hat{T}$ Approximate Solution for Temperature
U Velocity Vector
(u, v) Velocity Component in the x and y-axis
γ Coefficient of Convective Term
Γ_i Boundary of Subdomain Ω_i ($i=1$ and 3)
Γ_{2U} Inlet (Upstream) Boundary of Ω_2
Γ_{2D} Outlet (Downstream) Boundary of Ω_2
ρ Density of Lubricant
μ Dynamic Viscosity
Ω_i Three Subdomains ($i=1, 2, 3$)

Manuscript Received on November 8, 1982.
* Member DT Naval Ship Research and Development Center. Currently Visiting Professor at Seoul National University.

Introduction

The main objective of the present DTNSRDC ongoing research in the Tribology Program at DTNSRDC is to develop a reliable tool to predict the behavior of thrust bearings used in naval vessels over a wide range of operating conditions, with regard to both hydrodynamic and boundary lubrication. The first step toward this goal is to improve the hydrodynamic lubrication prediction. In this first-step approach, an immediate improvement over previous investigations is a full coupling of the thermal energy equation in the lubricant and the heat diffusion in the surrounding bearing and the collar. In this approach, a temperature variation is allowed across the lubricant film thickness and proper matching conditions are imposed on the interface boundaries between the lubricant and adjacent solids. In the present analysis, the standard thermal energy equation is parabolized by assuming that the ratio of the diffusion term to the convection term along the flow direction is of small order.

It has been known that for a parabolic-type partial differential equation an instability arises when the classical Galerkin method is applied, since this method is equivalent to the centered difference approximation. Probably the most extensively studied problem of this type is solution of the well-known boundary layer equations. In the boundary layer equations, most often a one-sided finite difference formula is used, which is equivalent to choosing the basis for the test function space to be different from that for the trial function space in the finite element method. There are many reports describing the introduction of various weighting functions in the inner product or the choice of a test function basis different (that is asymmetric) from the trial function basis [1~7]. The choice of a test function basis different from the trial function basis plays a role in controlling the degree of "upwinding" to maximize accuracy. Recently, extensive studies have been made for general convection-diffusion equations. However, rigorous investigations into the control of the degree of upwinding are limited to a simple one dimensional model problem with constant coefficients. For more general situations, maximization of accuracy by controlling the degree of upwinding is not straightforward. Therefore, it is desirable to have a simple numerical scheme which is uniformly stable over a wide range of values of the Peclet number.

In this report numerical results are obtained by the classical Galerkin method. The present numerical scheme gives uniformly stable results over a wide range of Peclet number for the paraboilzed thermal energy equation in the lubricant. The present numerical scheme is equivalent to the centered difference approximations for both the first and second derivative terms in the original differential equation.

Mathematical Modelling of the Problem

The computation domain consists of three rectangular subdomains, having heights H1, H2, H3, and length L as shown in Figure 1. However, the choice of actual boundary geometry is general (not necessarily rectangular domains) in the present method. The upper, middle, and lower subdomains are the bearing pad, the lubricant, and the bearing collar, denoted by Ω_1, Ω_2, and Ω_3, respectively. A rectangular co-ordinate system is used, the y-axis pointing upward and the x-axis pointing toward the right-hand side. The origin is taken at the mid-point of the left-hand side vertical boundary of the lubricant. The boundary of each subdomain is as shown in Figure 1,

$$\partial\Omega_i=\Gamma_i\cup J_i \qquad (i=1 \text{ and } 3)$$
$$\partial\Omega_2=\Gamma_{2U}\cup\Gamma_{2D}\cup J_1\cup J_2 \qquad (1)$$

Here the flow velocity U is also shown in Figure 1.

In the present numerical test, we ignore the convection term in the solids, i.e., Ω_1 and Ω_3, by assuming they are stationary. The thermal conductivity, $k_i (i=1,3)$ is assumed constant in each subdomain. In the subdomain Ω_2 (the lubricant), the velocity distribution is specifed a priori, hence the heat generating source term $\Phi(x,y)$ is known. The density ρ and the specific heat C of the lubricant are also assumed to be constants in Ω_2. Furthermore

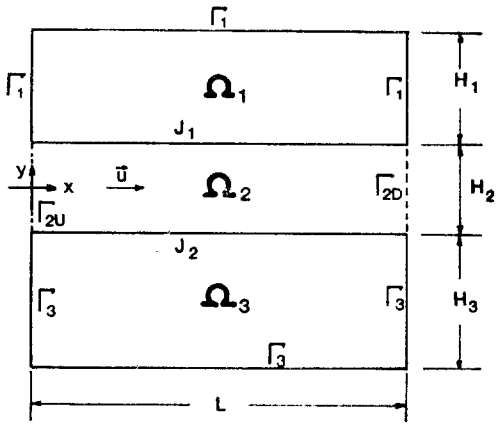

Fig. 1. Boundary Configurations

we assume that the diffusion term is much smaller than the convection term along the x-axis, and that the convection term is much smaller than the diffusion term in the y-axis. From these assumptions the original thermal energy equation, of an elliptic type in the lubricant, can be paraboized as follows. Let the temperature $T_i(i=1,2,3)$ be defined in each corresponding subdomain Ω_i. Then the thermal energy equation in each suadomain can be written as

$$-k_i\nabla^2 T_i=0 \quad \text{in } \Omega_i,\ (i=1 \text{ and } 3)$$
$$-k_2\frac{\partial^2 T_2}{\partial y^2}+\gamma\frac{\partial T}{\partial x}=\Phi(x,y) \quad \text{in } \Omega_2 \qquad (2)$$

where $\gamma=C\rho u$, and $\Phi=\mu\left(\frac{\partial u}{\partial y}\right)^2$ and μ is the dynamic viscosity. As mentioned before we assumed that the term $\left|k_2\frac{\partial^2 T_2}{\partial x^2}\Big/C\rho u\frac{\partial T_2}{\partial x}\right|=o(1)$ and $\left|C\rho v\frac{\partial T_2}{\partial y}\Big/k_2\frac{\partial^2 T_2}{\partial y^2}\right|=o(1)$ in the thermal energy equation in Ω_2, where u and v are, the velocity components along the x-axis and y-axis, respectively.

Since the thermal energy equation in Ω_2 is parabolized, we impose the boundary condition only on the upstream boundary, Γ_{2U}, and proper juncture conditions on J_1 and J_2, i.e.,

$$T_2=T_0 \quad \text{on } \Gamma_{2U} \qquad (3)$$

where the temperature of incoming lubricant, T_0, is specified. At the juncture surfaces J_1 and J_2 we require continuity of the temperature and its normal heat flux, i.e.,

$$T_1=T_2 \text{ and } k_1T_{1y}=k_2T_{2y} \text{ on } J_1$$

and

$$T_2=T_3 \text{ and } k_2T_{2y}=k_3T_{3y} \text{ on } J_2 \qquad (4)$$

In the first numerical model problem, the following three standard types of boundary conditions on Γ_1 and Γ_3 are treated specifically for testing numerical convergence:

(i) Dirichlet type;

$$T_i=T_0 \text{ on } \Gamma_i\ (i=1 \text{ and } 3) \qquad (5)$$

where T_0 is specified.

(ii) Neumann type;

$$k_i\frac{\partial T_i}{\partial n}=f_i(x,y) \quad \text{on } \Gamma_i(i=1 \text{ and } 3) \qquad (6)$$

where $f_i(i=1 \text{ and } 3)$ is specified.

(iii) Robin type;

$$k_i\frac{\partial T_i}{\partial n}+h_iT_i=h_iT_0 \text{ on } \Gamma_i(i=1 \text{ and } 3) \qquad (7)$$

where the heat transfer film coefficient $h_i(i=1$ and 3) and the ambient oil temperature distribution $T_0(x,y)$ along Γ_1 and Γ_3 are specified. Here we assume the boundaries, Γ_1 and Γ_3 are in an oil bath with an ambient oil temperature $T_0(x,y)$. It should be noted here that the boundary condition on the downstream boundary (outlet) of lubricant, Γ_{2D}, is not specified but is obtained as a part of the solution. This is because the original elliptic equation has been reduced to a parabolic equation.

For the purpose of the error and convergence test in the first model problem, we take $H_1=H_2=H_3=2$, $k_1/k_2=3$, $h_1=h_3=1$, and the juncture boundaries J_1 and J_2 are $y=\pm1$, respectively. We begin with the exact solution given by a simple polynomial function in each subdomain as follows;

$$T_1(x,y)=-2x^2+x+2y^2-3y+3 \quad \text{in } \Omega_1$$
$$T_2(x,y)=-2x^2+x+y^2+y \quad \text{in } \Omega_2$$
$$T_3(x,y)=-2x^2+x+2y^2+\frac{11}{3}y+\frac{5}{3} \quad \text{in } \Omega_3 \qquad (8)$$

From a given arbitrarily specified function of γ, one can easily compute the heat generation Φ by Eqs (2) and (8) as

$$\Phi(x,y)=\gamma(4x-1)+2 \qquad (9)$$

The three different types of boundary conditions in model problem are computed from the known exact solutions given in Eq(8). For example, with the Robin type condition, $h_i=1$ $(i=1,3)$, $T_0(x,y)$ was computed from Eq(8) as

$$T_0=\frac{k_i}{h_i}\frac{\partial T_i}{\partial n}+T_i \quad \text{on } \Gamma_i,\ (i=1 \text{ and } 3)$$

and

$$T_0=y^2+y \qquad \text{on } \Gamma_2 U \tag{10}$$

In the second model problem, we only treat the Robin boundary condition on Γ_1 and Γ_3 to simulate a more realisitic experimental condition. For this case, the geometry of the bearing pad and collar and the lubricant film thickness are chosen as an analogous model in two dimensions corresponding to the three-dimensional experimental condition.

Galerkin's Method and Numerical Procedure

Before we describe Galerkin's finite method applied to the model problem formulated in the previous section, it is convenient to introduce a single continuous temperature function $T(x,y)$, defined in the entire domain, $\Omega=\Omega_1\cup\Omega_2\cup\Omega_3$, as follows;

$$T(x,y)=T_i(x,y) \text{ in } \Omega_i \ (i=1,2,3). \tag{11}$$

To construct the bilinear functional in weak form, we first introduce the test function T^* in the test function space, and next define the inner product of the original partial differential equations in (2) and the test function T^*. By integrating by parts the inner product reduces to

$$\begin{aligned}&\iint_{\Omega_1} k_1\nabla T\nabla T^*dxdy+\iint_{\Omega_2} k_2\frac{\partial T}{\partial y}\frac{\partial T^*}{\partial y}dxdy\\&+\int_{\Omega_3} k_3\nabla T\nabla T^*dxdy+\int_{\Gamma_1} h_1TT^*ds+\int_{\Gamma_3} h_3TT^*ds\\&+\iint_{\Omega_2}\gamma\frac{\partial T}{\partial x}T^*dxdy=\iint_{\Omega_2}\Phi T^*dxdy\\&+\int_{\Gamma_1} h_1T_0T^*ds+\int_{\Gamma_3} h_3T_0T^*dl\end{aligned} \tag{12}$$

where the trial function $T^*=0$ on $\Gamma_2 U$, and the trial function T is chosen so that the essential condition $T=$To on $\Gamma_2 U$ is satisfied. Eq (12) is a weak from form for the Robin condition. For the Dirichlet type condition on Γ_1 and Γ_3, the integrals along Γ_1 and Γ_3 in Eq (12) are not present. On the other hand the trial function should satisfy the Dirichlet conditions and the test function is chosen to be zero on Γ_1 and Γ_3. In the case of the Neumann type condition, the boundary integrals along Γ_1 and Γ_3 appearing on the left-hand side of Eq (12) should not be present and h_i To in the integrands of the boundary integrals along Γ_1 and Γ_3, on the right-hand side of Eq (12), should be replaced by $f_i(x, y)$, $(i=1$ and $3)$.

It is of interest to note that the juncture conditions on J_1 and J_2 given in Eq (4) are satisfied as natural conditions in Galerkin's functional equation given above. In the numerical computations an isoparametric linear element is used as the basis for both trial and test functions throughout the present computations. This choice of basis function is equivalent to the centered fiinte difference approximation. In a straightforward manner, the bilinear form in Eq (12) is reduced to a set of algebraic equations. The coefficient matrix obtained is not symmetric but still has a banded structure. The asymmetry is duc to the presence of the convective term in a subdomain. The Gaussian elimination method is used is used to solve the reduced matrix equation.

Numerical Convergence Test in the First Model

An extensive numerial test of the convergence has been made in the first model problem. To test numerical convergence of the present numerical scheme, we define the error, $E_i(i=1,4)$, in four different ways using the known exact solution T given in Eq (8) and the finite element numerical solution $\hat{T}(x,y)$ as follows:

$$\begin{aligned}E_1&=\|T-\hat{T}\|_\infty\\E_2&=\left\{\iint(T-\hat{T})^2dxdy+\iint k[\nabla(T-\hat{T})]^2dxdy\right\}^{1/2}\\E_3&=\|\nabla(T-\hat{T})\|_2\\E_4&=\|T-\hat{T}\|_2\end{aligned} \tag{13}$$

where $\|\ \|_\infty$ and $\|\ \|_2$ are the well-known max norm and L_2 norm, and defined as

$$\begin{aligned}\|T-\hat{T}\|_\infty&=\max_{(X,Y)\in\Omega}|T-\hat{T}|\\\|T-\hat{T}\|_2&=\left\{\iint(T-\hat{T})^2dxdy\right\}^{1/2}\end{aligned} \tag{14}$$

and where $k=k_i$ in Ω_i $(i=1,2,3)$

In the finite element mesh subdivisions, $\Delta x/\Delta y=1$ is used throughout the first model problem, where Δx, and Δy are the lengths of the finite element along the x- and y- axes respectively (i.e., a square element is used for this model problem). Ten different sizes of uniform square elements are tested in the range of $2\leqslant L/\Delta x\leqslant 20$. The specific mesh-

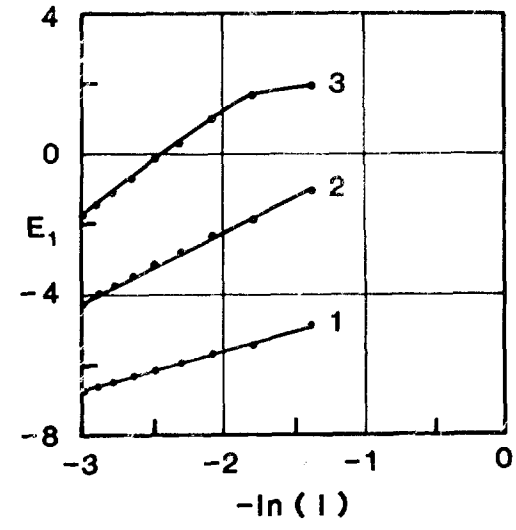

(a)

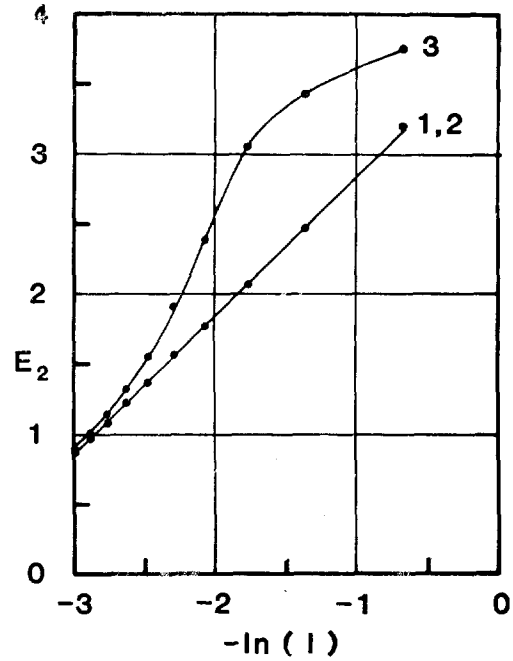

(b)

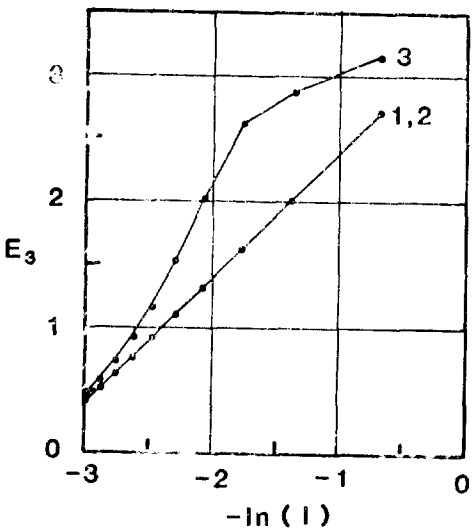

(c)

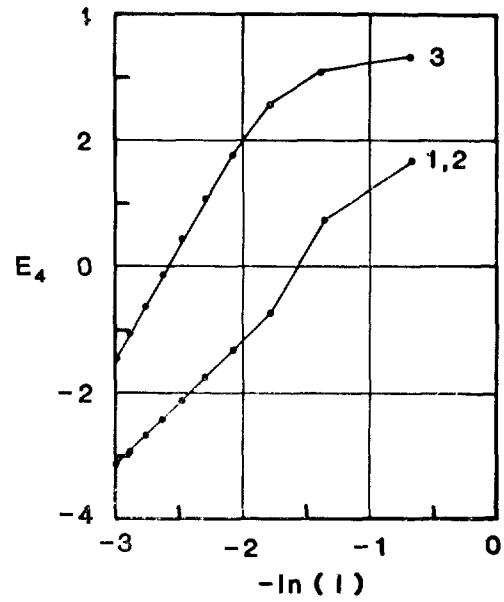

(d)

Fig. 2. Error covnergence test results for the Robin condition.
In Figure 2 through Figure 4, the following legends are used:
(a),(b),(c),(d) are the results of $E_1.E_2,E_3$, and E_4, respectively (see Eq 13) The ordinate scale is the same in all figures. The curves designated by 1, 2, and 3 correspond to the case of P_e=0.01, 1, and 100, respectively.

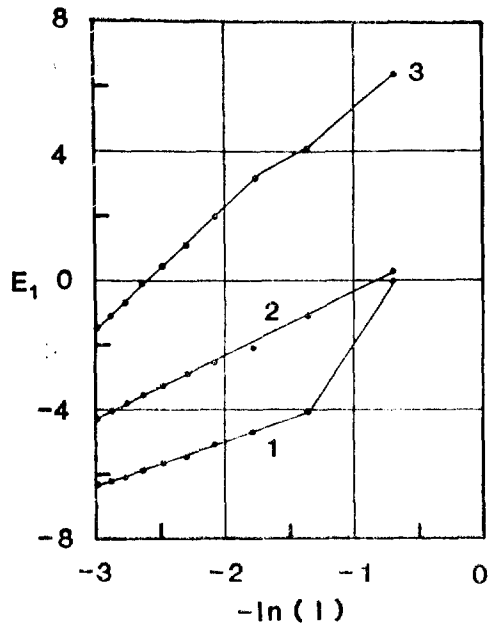

(a)

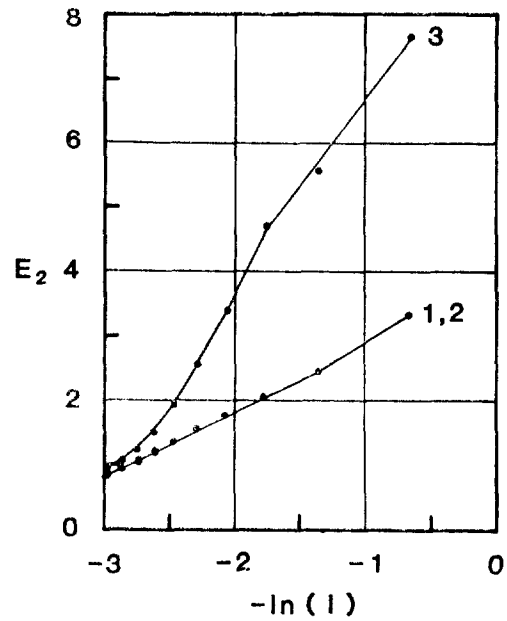

(b)

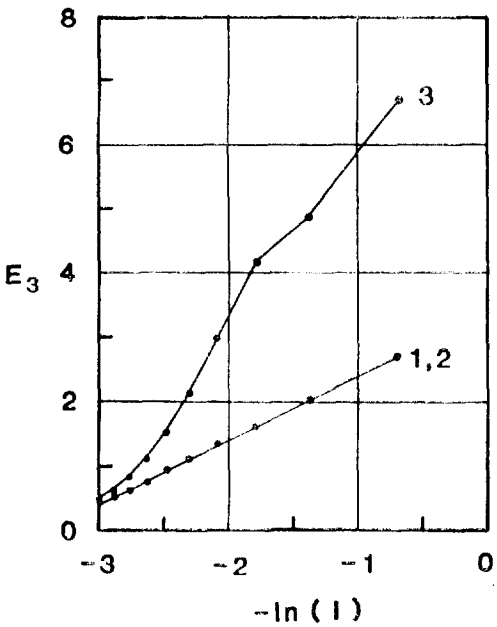

(c)

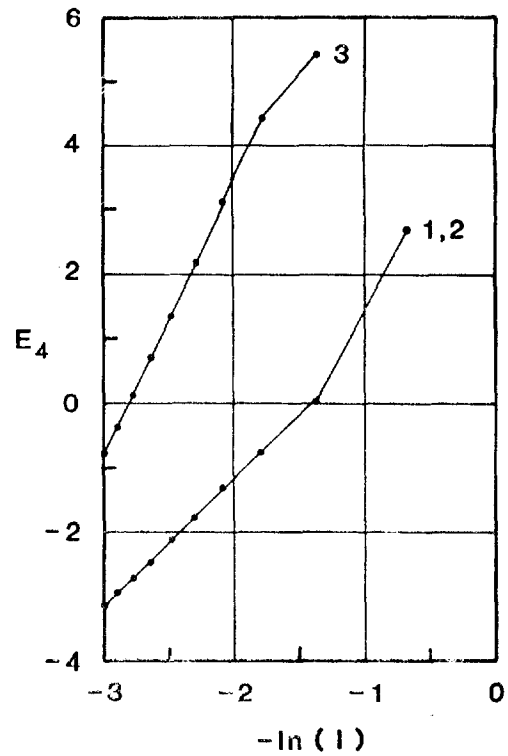

(d)

Fig. 3. Error convergence test results for the Neumann condition. (See Figure 2 for the legend)

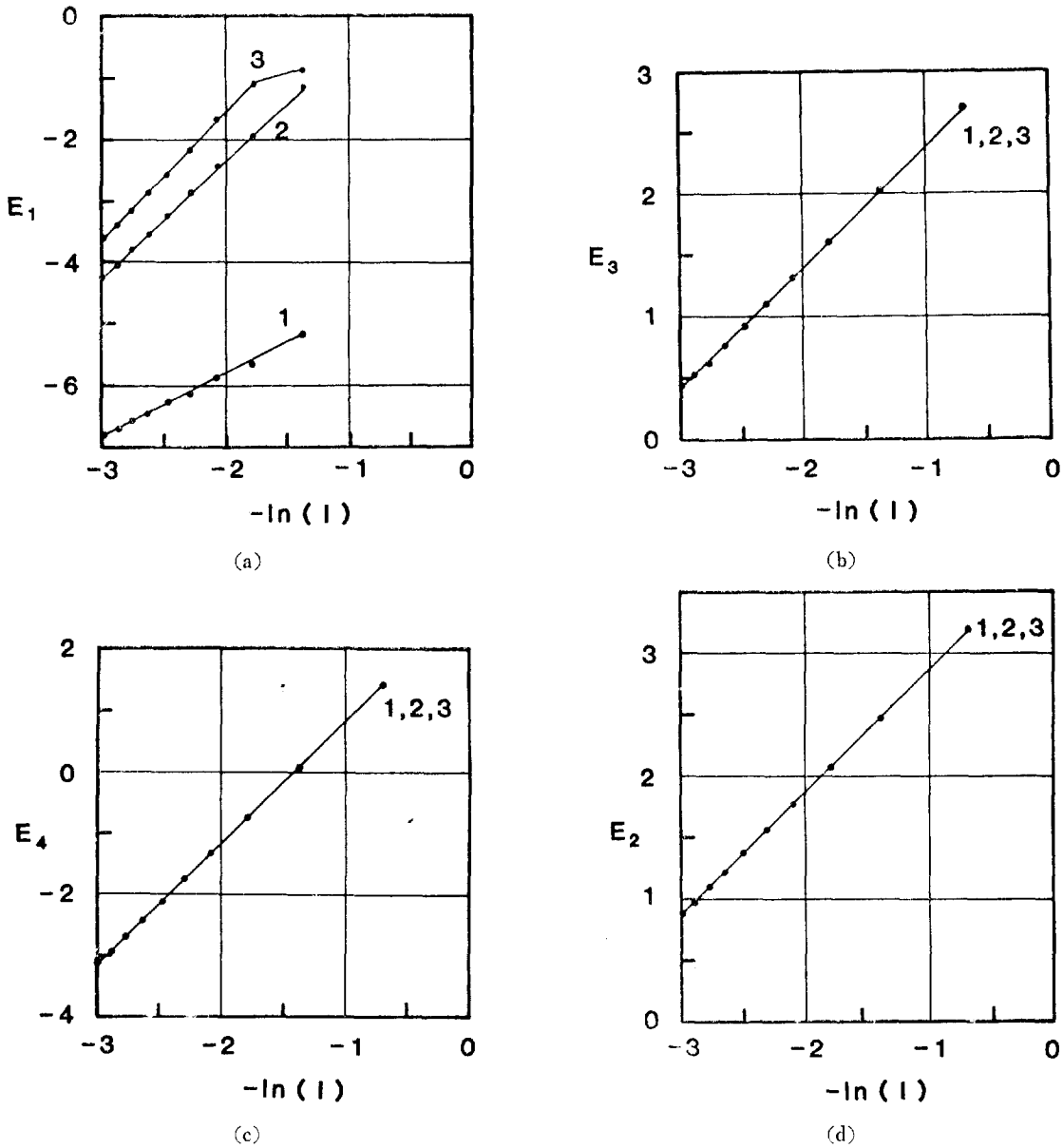

Fig. 4. Error convergence test results for the Dirichlet condition. (See Figure 2 for legend)

subdivisions tested are given in Table 1. In the present model problem, the computations are made for three values of Peclet number: $Pe=\gamma H_2/2=0.01$, 1, and 100.

If we assume that the error behaves like $E_i \propto (\Delta x)^n$ $(i=1, 2, 3. 4)$ as the limit $\Delta x \to 0$, then we may represent the error as

$$E_i = A(1/I)^n, \tag{15}$$

where A is constant and I is defined in Table 1. By taking the log of Eq (15), we obtain

$$\ln E_i = \ln A - n \ln I \tag{16}$$

From our numerical results for ten different finite-element mesh subdivisions, we have plotted the curve of the points ($-\ln I$, $\ln E_i$) shown in Figs. 2 through 4. From the two finest finite element subdivisions, the values of index n and the constant A are obtained for three different values of the Peclet number, Pe, and also for three types of

Table 1. Ten different finite element subdivisions used for the error test.

Test case(i)	1	2	3	4	5	6	7	8	9	10
I	2	4	6	8	10	12	14	16	18	20
J	3	6	9	12	15	18	21	24	27	30
EL	6	24	54	96	150	216	294	384	486	600
N	12	35	70	117	176	247	330	425	532	651
MB	9	17	23	29	35	41	47	53	59	65
DIM	108	595	1,610	3,395	6,160	10,127	15,510	22,525	31,388	42,315

I =Number of element along the x-axis
J =Nnmber of element along the y-axis
EL=Totai number of elements
N =Total numal number of nodes
MB =Bandwidth (asymmetric)
DIM=Core memory space for the coefficient matrix

Table 2. The Values of n in various Error Norms for Three Peclet Numbers, P_e.

Boundary Condition	P_e	E_1	E_2	E_3	E_4
Robin	0.01	1.0038	1.0004	1.0000	2.0000
	1	2.0607	1.0004	1.0000	1.9971
	100	3.2114	1.1082	1.1482	3.7273
Neumannn	0.01	1.2871	1.0004	1.0000	1.9985
	1	2.0098	1.0004	1.0000	1.9834
	100	3.6481	1.3138	1.3709	4.1813
Dirichlet	0.01	.9175	1.0004	1.0000	2.0000
	1	2.0366	1.0003	.9999	2.0003
	100	2.1011	1.0009	1.0008	1.9957

Table 3. The Values of Constant A in various Error Norms for Three Peclet Numbers, P_e.

Boundary Condition	P_e	E_1	E_2	E_3	E_4
Robin	0.01	.2481E−01	.4761E+02	.2993E+02	.1721E+02
	1	.7006E+01	.4769E+02	.3005E+02	.1726E+02
	100	.2580E+04	.6760E+02	.4908E+02	.1601E+05
Neumann	0.01	.8260E−01	.4761E+02	.2993E+02	.1740E+02
	1	.5876E+01	.4769E+02	.3005E+02	.1641E+02
	100	.1299E+05	.1281E+03	.9813E+02	.1257E+06
Dirichlet	0.01	.1740E−01	.4761E+02	.2993E+02	.1702E+02
	1	.6339E+01	.4768E+02	.3004E+02	.1747E+02
	100	.1472E+02	.4823E+02	.3085E+02	.1866E+02

boundary conditions on Γ_1 and Γ_3. The results are given in Table 2 and 3. In Table 2 the values of n for E_1 and E_3 are almost one, i.e., the corresponding convergence error is linear, as a function of $(I)^{-1}$ for all three types of bounditions all three Peclet numbers tested except for Pe=100 in the Neumann boundary condition. It is surprising to see that the the convergence of the E_1 error is accelerated as the Peclet number increases · this is contrary to our expectation.

It is contrary to our expectation. It is also difficult to draw any conclusion on the behavior on the convergence of the error E_1 as the Peclet number increases.

In Table 3. the constant A for E_1 increases as the Peclet number increases with all three types of boundary conditions on Γ_1 and Γ_3. However, the constant A for E_2 and E_3 does not vary much for all three types of boundary conditions and for the three values of Peclet numbers.

From the results shown in Figure 3 and Table 2 and 3, the present numerical evidence shows uniform convergence of the present numerical scheme. However, a rigorous mathematical error analysis and convergence proof is still open for the class of parabolic-elliptic coupled problem treated here.

Results for a Second Model Problem

For the second model problem, the following geometrical and material data are used:

$H_1=H_3=0.75$ inch
$H_2=0.001$ and 0.0001 inch
$L=2.5$ inch
$u_0=9.55$ inch/sec and 47.75 inch/sec
$C=0.5$ Btu/lbm/°F
$k_1=k_3=26$ Btu/hr/ft/°F
$k_2=0.075$ Btu/hr/ft/°F
$T_0=100$°F
$h_1=h_3=30$ Btu/hr/ft²/°F
$a=6.5\times10$ lbm.sec/in
$\rho=0.84\times10$ lbf sec/in
$J=9336$ in.lbf/Btu

where u_0 is the maximum velocity in the lubricant film. The value of Φ is approximated by

$$\Phi(x, y)=\mu\left(\frac{\partial u}{\partial y}\right)^2\doteq\mu\left(\frac{u_0}{H_2}\right)^2$$

and γ is computed by using the mean velocity, i.e., $u=u_0/2$, since the velocity is assumed linear between zero on J_1 and u_0 on J_2.

If all the dimensional quantities are converted to consistent dimensions using (Btu, sec, in, °F), then the following values of coefficients are obtained for use in Eqs (2) and (7):

$$k_1=k_3=602\times10^{-6}\ \frac{Btu}{sec\ in^2\ °F/in}$$

$$k_2=1.74\times10^{-6}\ \frac{Btu}{sec\ in^2\ °F/in}$$

$$h_1=h_3=57.87\times10^{-6}\ \frac{Btu}{sec\ in^2°F}$$

Table 4. Four tested cases for the values of γ and Φ.

Case No.	H_2(inches)	u_0(inch/sec)	γ(Btu/sec/in/°F)	Φ(Btu/in/sec)
1	0.001	9.550	0.0810	0.06427
2	0.001	47.750	0.0405	1.6070
3	0.0001	9.550	0.0810	6.4270
4	0.0001	47.750	0.0405	160.7000

Table 4 shows four specific test conditions, which are the combinations of two velocities and two film thickness.

In the present computations, two different sets of mesh subdivisions are used; the first set of data with a coarse mesh has 77 nodes and 60 elements. The second set of data with a fine mesh has 315 nodes and 280 elements. In the fine mesh, we took four uniform rectangular elements in the lubricant (Ω_2)

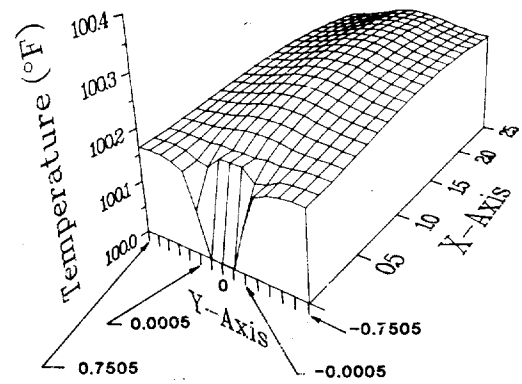

Fig. 5. Temperature distributions for Case 1. $H_2=0.001$ inch, $u_0=9.55$ in/sec

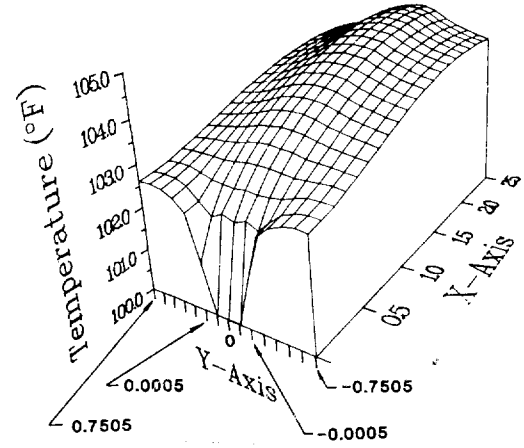

Fig. 6. Temperature distributions for Case 2. $H_2=0.001$ inch, $u_0=47.75$ in/sec

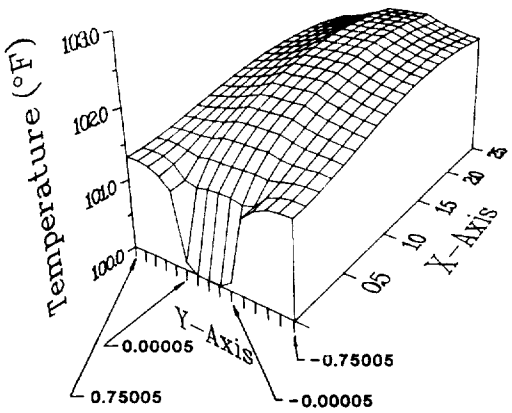

Fig. 7. Temperature distributions for Case 3. $H_2=0.0001$ inch, $u_0=9.55$ in/sec

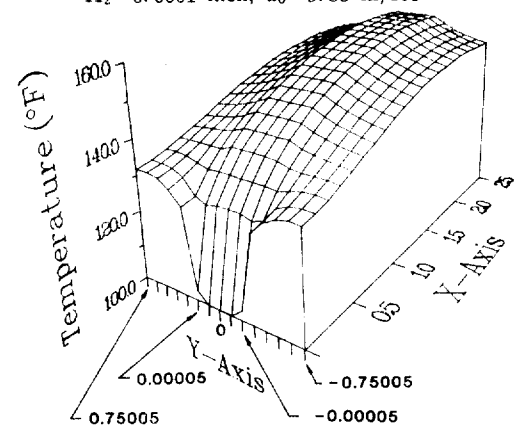

Fig. 8. Temperature distributions for Case 4. $H_2=0.0001$ inch, $u_0=47.75$ in/sec

and five uniform rectangular elements in both bearing pad and collar (Ω_1 and Ω_3) along the y-axis, and twenty elements along the x-axis.

The agreement between the computed temperatures obtained by a fine mesh and a coarse mesh was good. Therefore only the results obtained by using the fine mesh are shown in Fig. 5 through 8. In this three dimensional computer plot of the temperature distribution, a total of 315 nodes were used with linear interpolation. It should be noted here that the film thicknesses (i.e., 0.001 and 0.0001 inches) were stretched very much along the y-axis for better illustration in the computer plots.

The results for all four cases show that the effect of the inlet temperature (100°F is used here) is limited to a small local region around the inlet. This result shows that there exists a very thin thermal boundary layer at the inlet (i.e., the initial layer in the time-dependent problem). This results is not surprising, since the heat is generated only in the lubricant.

It is of interest to note that for all four cases, the temperature T at the second node on the boundary J_1 (or J_2) from the inlet (Γ_{2v}, $x=0$) is lower than that at the adjacent node inside the solids(i.e., Ω_1 or Ω_3). This means that there is a small region of local backflow of heat flux. In other words, in this region, the heat flux vector is pointing from the point in the solid to the lubricant, even though the only heat generating source in this problem is in the lubricant region.

Concluding Remarks

From the numerical results presented for the first model lubrication problem, we can conclude that the seemingly-unstable classical Galerkin method is uniformly stable over the range of the Peclet number from 0.01 to 100. This stability is problably a result of the subdomain of the parabolic equation being sandwiched between two adjacent subdomains which are elliptic without a convective term in the heat transfer equations. It appears that the elliptic type equations for the top and bottom subdomains play a role in stabilizing the numerical scheme even though we use the classical Galerkin method which is equivalent to the centered finite difference approximation. In the second model problem, a local backflow of the heat flux and the presence of the thermal boundary layer are illustrated. Future work should include the convective term in the bearing collar where numerical stability may not result using the present method, unless a proper weighting function is introduced in the inner product.

Acknowledgment

The author is very grateful to Professor Coda Pan, Columbia University and Mr. Thomas L. Daugherty, and Dr. James Ma, David W. Taylor

Naval Ship R&D Center, for many helpful discussions and continuous guidance through monthly meetings. The help of Mr. R. Privette for the computer plot is also appreciated.

References

[1] Axelsson, O., "Stability and Error Estimates of Galerkin Finite Element Approximations for Convection-Diffusion Equations," IMA Journal of Numerical Analysis, Vol. 1, pp. 329-345, 1981.

[2] Christie, I., D.F. Griffiths, A.R. Mitchell and O.C. Zienkiewicz, "Finite Element Methods for Second-Order Differential Equations with Significant First Derivatives," Int. J. Num. Methods, Engnr, Vol. 10, pp. 1389-1396, 1976.

[3] Christie, I. and A.R. Mitchell, "Upwinding of High Orrder Galerkin Methods in Conduction-Convection Problems," Int. J. Num. Meth. **Engnr, Vol.** 12, pp. 1764-1771, 1978.

[4] Heinrich, J.C., P.S. Huyakorn, O.C. Zienkiewicz and A.R. Mitchell, "An Upwind Finite Element Scheme for Two-Dimensional Convective Transport Equation," Int. J. Num. Meth. Engnr, Vol. 11, pp. 131-143, 1977.

[5] Hughes, T.J.R., "A Simple Scheme for Developing 'Upwind' Finite Elements," Int. J. Num. Meth. Engnr, Vol. 12, pp. 1359-1365, 1978.

[6] Blackburn, W.S., "Letter to the Editor," Int. J. Num. Meth. Engnr, Vol. 10, pp. 718-719, 1976.

[7] Ben-Sabar, E. and B. Caswell, "A Stable Finite Element Simulation of Convective Transport," Int. J. Num. Meth. Engnr, Vol. 14, pp. 545-565, 1979.